Full-Field Measurements of Fracture Initiation and Crack Growth in Superelastic Nitinol

Kenneth E. Perry and Paul E. Labossiere
ECHOBIO LLC
Bainbridge Island, WA.

Abstract

We present results for full field measurements of crack tip deformation fields in Nitinol using high sensitivity Moiré Interferometry. Three fatigue loading scenarios are examined illustrating the effect of stress induced martensite transformations at the tip of the crack. Understanding the behavior of fatigue crack growth is paramount to the successful use of this highly complex material response, especially for such application as implantable medical devices. The results demonstrate the sensitivity of heterogeneous phase transformations on the crack growth behavior.

Introduction

With the increasing use of Nitinol in medical implants, there is a need for improved characterization of the material behavior of Nitinol and methodologies for better product design and engineering. The typical approach of employing the force-deformation response from uniaxial tension tests for input and validation of material models is rather limited. Especially when trying to extend simplified approaches of traditional fatigue and fracture mechanics to identify appropriate "material limits" and validate design life. Limited published work has been done in this area, including the work by Ritchie, et.al. 1999, 2007.

Methodology

Phase shifted moiré interferometry was used to observe the initiation and growth of short cracks in Nitinol C(T) samples. The samples were produced using material and processes typical for implantable medical devices. Well characterized materials and a range of processing conditions were studied using typical LEFM and EPFM fracture test methods while recording the details interferograms.

Three primary loading conditions were studied to characterize the fracture behavior of Nitinol. "A" loading refers to elastic loading and unloading of the austenite phase only, "M" loading" refers to elastic loading and unloading of the martensite phase only and "AM" loading refers to both phases being present, forward/reverse transformations.

The samples were tested under load control with direct feedback between the recorded fringe information and the dynamic load actuator. This permitted exceptional visual/interferometric crack length measurements, the observation of complex time-dependent material behavior and the evolution of crack tip strain fields. Full-field displacements at Kmax, Kmin and K = 0 were obtained automatically during cyclic fatigue testing to generate time lapse deformation and crack growth histories for the range of materials and processing considered.

Comparisons were made between initiating conditions and during the evolution of crack tip fields to better understand the application of fatigue and fracture methodologies to the design and testing of implantable medical devices.

Set-up

The specimens were made from Superelastic Nitinol with an Af < 20°C from two different material sources with different processing histories. Standard compact tension specimens 12.5mm square and 1.5mm thick were laser cut from the material and successively sanded and polished flat down to 1 micron diamond paste. The moiré diffraction gratings with 300 lines per mm were photolithographic replicated onto the surface of the specimens ensuring that there were as thin as possible. The custom built portable custom 4-beam phase shifted moiré interferometer images were captured using a 1280x960 10 bit grayscale camera with an 8x optical zoom lens with real-time data acquisition and control.

The specimens were subjected to cyclic fatigue loading with a Bose 3200 ElectroForce test system under either displacement, load and user channel control and integrated with psmi DAQ system. The load capacity and rate for sub-critical testing was matched to the characteristics of the specimens prior to testing using finite element analysis and calibration the details of which are not shown here. These calculations provided a first estimate the mean and alternating load conditions required to obtain various material states in the vicinity of the crack tip. Figure 1 shows two photographs of experimental set-up showing 4-beam phase shifted moiré interferometer and specimen mounted in the Bose 3200 ElectroForce test system. Figure 2 shows wrapped fringe patterns illustrating the advantage of phase shifting and the exceptional grating quality and spatial resolution.

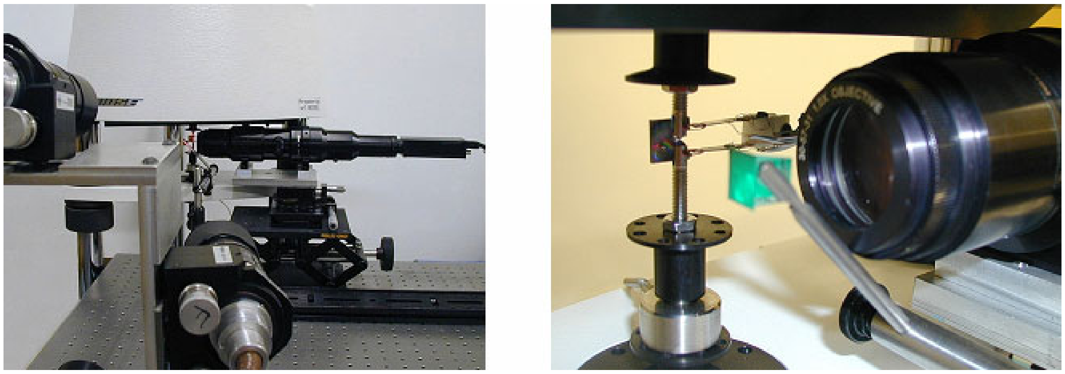

Figure 1. Photographs of experimental set-up showing 4-beam phase shifted moiré interferometer and specimen mounted in the Bose 3200 ElectroForce test system.

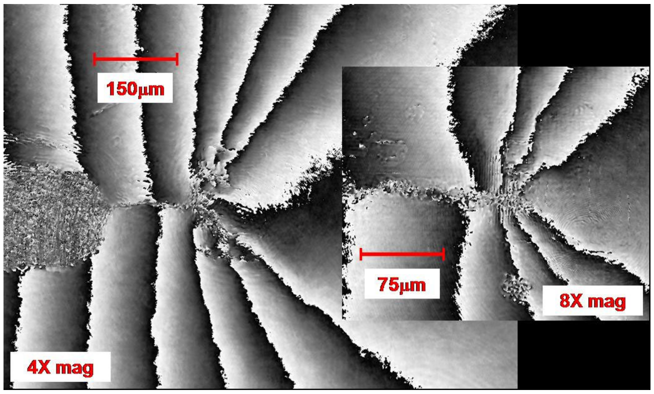

Figure 2. Wrapped fringe patterns showing the exceptional fringe quality and the spatial resolution.

Discussion

Three cyclic load scenarios were explored referred to as A loading, M loading and AM loading reflecting the state of the material at the tip of the crack as either Austenite (no martensite transformation, fully austenite crack tip zone achieved at low mean loads), Martensite (stable martensite crack tip zone achieved at higher mean loads) or Austenite to Martensite stress induced transformation (transformation reversal from maximum to minimum loading achieved at high alternating loads). These different conditions were obtained by altering the magnitude of the mean and alternating load applied to the specimen and monitoring the resulting crack tip fields. For the A Loading in the linear region, no transformation or wake effects are observed as was expected and initiation and propagation occur in a consistent and uniform fashion. Figure 3 shows wrapped fringes and fringe masks showing stable and consistent crack tip behavior during A loading at maximum and minimum load. There is no stress induced martensite transformation at the tip of the crack and the stress fields are consistent with those observed in traditional linear elastic materials. For both the AM and M loadings with transformation influence, wake effects can be observed resulting in non-consistent transformation zones that develop.

Figure 4 shows fringe masks showing further growth of a previously pinned crack tip during M loading. The transformation zone is clearly visible by the dark regions due to loss of fringe coherence at the tip of the crack.

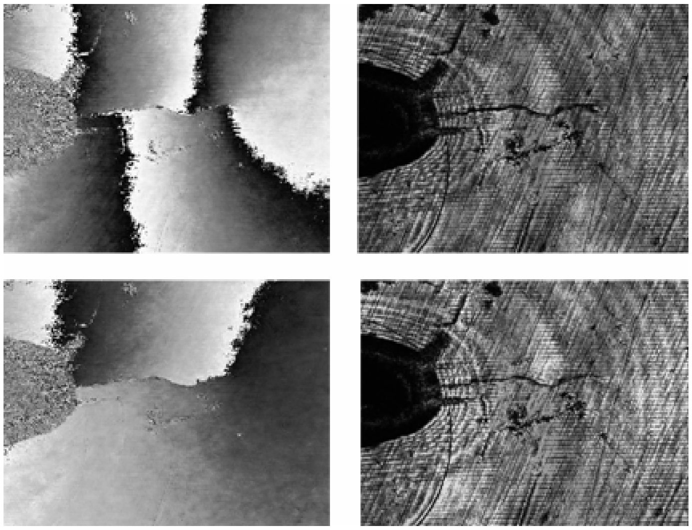

Figure 3. Wrapped v-field fringes and fringe masks showing stable and consistent crack tip behavior during A loading at maximum load (upper) and minimum load (lower).

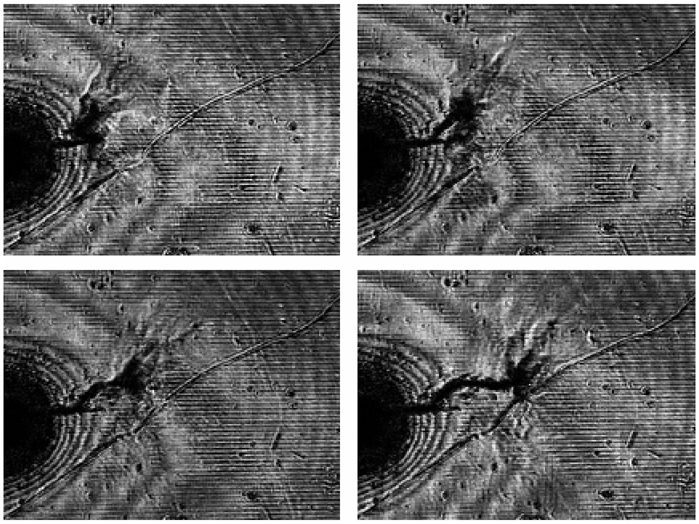

Figure 4. Fringe masks showing further growth of a previously pinned crack tip at mean load during M loading.

For AM loading, the behavior is even more unstable with the typical observation of unsymmetrical and non-consistent transformation zones as shown in Figure 5. Figure 6 shows another transformed zone during AM loading.

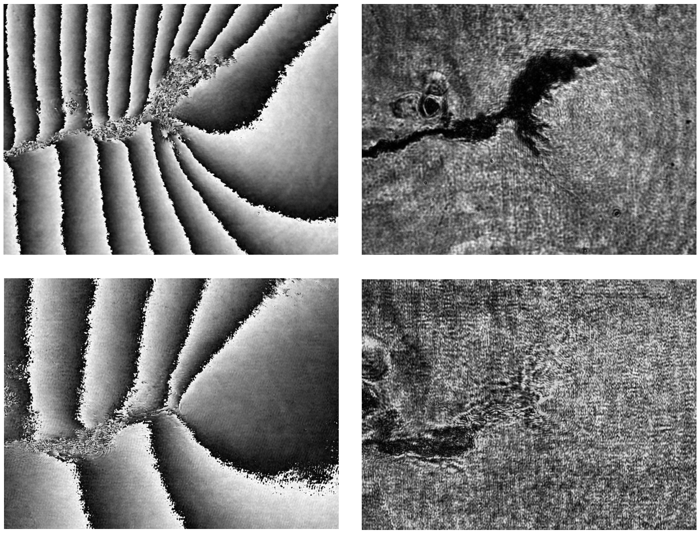

Figure 5. V-field of loading (top) and unloading (bottom) with transformation (AM Loading)

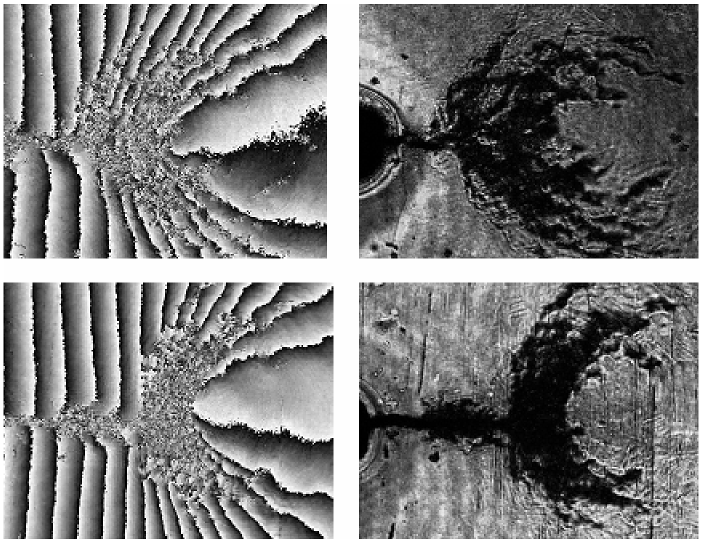

Figure 6. Initiating the crack at a high Kmax (top) and growing the crack at a decreased Kmax (bottom) clearly showing the wake effect and the residual in the v-fields.

Pinning and bifurcations from interruptions in testing are clearly visible in the post crack zone. This pinning phenomenon is mostly due to transformation/temperature coupling and potential due to microstructural obstacles. Size effects can be resolved in the different test protocols with the transformation zone size being relative to notch and crack sizes. For short cracks, the notch-tip fields control the transformation zone size, whereas for long cracks, the crack tip fields control the transformation zone size.

Crack initiation and growth in Nitinol is far more complex than traditional engineering materials. Heterogeneous phase transformations and localizations result in a far more complex stress and strain state at the tip of the crack that are not described by the typical LEFM or even EPFM crack tip fields. Crack path tortuousity, deflection, and pinning of the crack due to the transformation response depend significantly on the mean loading and illustrate the load history and dependence on the response of crack initiation and growth in Nitinol. This behavior is complicated by the thermal sensitivity and transformation temperature coupling effects which make the stress-strain response highly rate dependant and dynamic with cyclic loading.

This complex behavior makes the identification of useable material limit data difficult and traditional threshold crack growth rates can not be directly applied, especially to medical devices.

Acknowledgements

The authors would like to thank Eric Steffler, Randy Lloyd and others at the Idaho National Engineering Laboratory, Scott Andersen of BOSE/Enduratek for the use of the Bose 3200 ElectroForce test system, Frank Sczernie of Special Metals for materials and characterization, LaserAge and NDC for prototype services.

References

McKelvey and Ritchie R.O., Fatigue-crack propagation in Nitinol, a shape-memory and superelastic endovascular stent material, *Journal of Biomedical Materials Research*, Volume 47, Number 3, Pages 301-308, 1999

Robertson S.W. and Ritchie R.O., In vitro fatigue–crack growth and fracture toughness behavior of thin-walled superelastic Nitinol tube for endovascular stents: A basis for defining the effect of crack-like defects, *Biomaterials*, Volume 28, Issue 4, pages 700-709, 2007